



Anomalous SST warming during MIS 13 in the Gulf of Lions (northwestern Mediterranean Sea)



Aleix Cortina^{a,*}, Joan O. Grimalt^a, Belen Martrat^a, Andrés Rigual-Hernández^b, Francisco Javier Sierro^c, José Abel Flores^c

^a Department of Environmental Chemistry, IDAEA-CSIC, 08034 Barcelona, Spain

^b Department of Biological Sciences, Macquarie University, North Ryde, NSW 2109, Australia

^c Department of Geology, University of Salamanca, 37008 Salamanca, Spain

ARTICLE INFO

Article history:

Received 27 September 2015

Received in revised form 2 December 2015

Accepted 5 December 2015

Available online 11 December 2015

Keywords:

Alkenone

MIS 13

Gulf of Lions

ABSTRACT

During the PROMESS campaign (summer 2004) a borehole (PRGL1) was drilled in the upper slope of the Gulf of Lions covering the last 530 kyr. Here, we present new biomarker data from 440–528 kyr in order to reconstruct past climate variability, sea surface temperature (SST) (alkenone-based) and oxygenation of the bottom waters (based on *n*-hexacosanol and *n*-nonacosane ratio) during Marine Isotope Stages (MIS) 12 and 13. Contrary to southern paleorecords, MIS 13 showed the warmest SST values of the past 530 kyr in the Gulf of Lions, which is in agreement with recent findings in northern continental paleorecords. Our data suggest that the ice volume in northern latitudes and its effect on Inter-Tropical Convergence Zone (ITCZ) position during winter caused the anomalous warming in the northwestern Mediterranean during MIS 13. Moreover, the northward incursion of the ITCZ could have modified the stadial reinforcement of north-westerly winds documented from MIS 11 to the present.

© 2015 Elsevier Ltd. All rights reserved.

1. Introduction

The MIS 13 has been the subject of recent studies due to the disagreement between southern and northern paleorecord reconstructions. Compared with the later interglacials, benthic $\delta^{18}\text{O}$ values of MIS 13 (478–533 kyr) (Lisiecki and Raymo, 2005) showed the heaviest values, which are usually interpreted as a signal of larger global ice volume. This view is in agreement with the Epica Dome C δD (EDC δD) records, where MIS 13 yielded the coolest interglacial temperatures of the 800 kyr (about 4 °C cooler than the Holocene; Jouzel et al., 2007). However, several continental records of the Northern Hemisphere contradict the idea of a cooler interglacial having a larger ice volume. For example, analysis of sediment cores from: (1) the Loess deposits in China (Vandenbergh, 2000; Sun et al., 2006; Guo et al., 2009), lower and middle Danube River (Fitzsimmons et al., 2012) and Serbia (Marković et al., 2009); (2) Greenland coast (de Vernal and Hillaire-Marcel, 2008) and (3) lakes of the Tibetan plateau (Chen et al., 1999) and Siberia (Prokopenko et al., 2002) suggest that

the conditions during MIS 13 were relatively warm and coupled with relatively low global ice volume.

The intensity of the north-westerly winds in the Gulf of Lions has been suggested to be influenced by the extension of the ice-sheets in the Northern Hemisphere (Kuhlemann et al., 2008; Cortina et al., 2011, 2013). The presence of large ice-sheets during Last Glacial Maximum (LGM) resulted in the southward displacement of the position of the polar front (Pflaumann et al., 2003) causing the invasion of Arctic air masses into the northwestern Mediterranean with a consequent decrease of sea surface temperatures (SST) in the Gulf of Lions (Kuhlemann et al., 2008). Therefore, the study of SST variations in the Gulf of Lions could be a good indicator of the northern ice-sheet variability. Here, we present new biomarker data from MIS 12 to MIS 13 of the core PRGL1 situated in the Gulf of Lions with the main goal to investigate the northern ice-sheet extension during MIS 13 and to provide new insights into the paleoclimatic conditions during this interglacial stage.

2. Study area

As part of the European Project PROMESS 1 (profiles across Mediterranean Sedimentary Systems), borehole PRGL1 (300 m

* Corresponding author.

E-mail address: acortina@usal.es (A. Cortina).

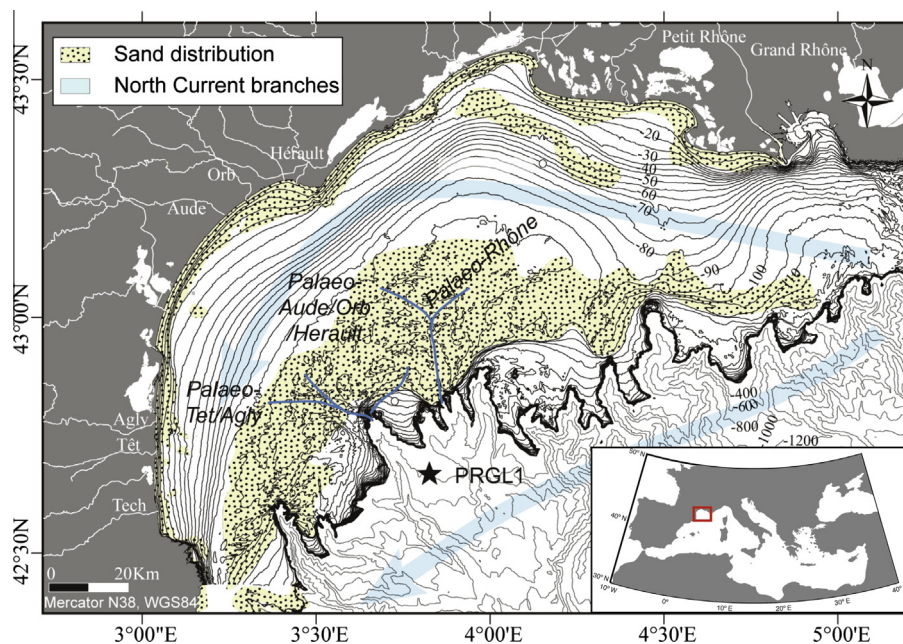


Fig. 1. Map of the Gulf of Lions taken from Jouet et al. (2006). The present-day morphology and the sand distribution on the continental shelf (Aloisi, 1986) illustrating the last glacial sea-level rise. Blue arrows depict the two North Current branches. Core site PRGL1 is indicated by a black star. (For interpretation of the references to color in this figure legend, the reader is referred to the web version of this article.)

length) was drilled in the upper slope of the Gulf of Lions (42.690° N, 3.838° E) (Fig. 1) on the interfluvial of the Boucart and Hérault canyons at a water depth of 298 m. The study site is very suitable for the preservation of continuous sedimentary records because: (1) there is a good balance between the sedimentation rates and the accommodation space; (2) it is not strongly influenced by the Rhône deltaic system and (3) it is distant from the Catalonian Margin, where strong erosive processes have been documented (Rabineau et al., 2005).

The general oceanographic circulation in the Gulf of Lions is governed by a cyclonic along-slope Northern Current (NC), which is divided in two branches: the principal branch flowing through the continental slope, and a secondary branch that penetrates the continental shelf (Millot, 1990) (Fig. 1). Due to seasonal stratification and changing wind regimes, the current oscillates in magnitude and direction over the year, doubling its intensity during winter compared to summer (Béthoux, 1984).

The study area is under the influence of the cool north-westerly winds (the Mistral and Tramontana), blowing through the Pyrenees, the Massif Central and the Alps. On a large scale, the north-westerly winds induce upwelling that spreads out over two-thirds of the gulf, and downwelling over one-third (Millot, 1982). Consequently, north-westerly winds are responsible for downwelling and upwelling processes simultaneously. The upwelling processes bring colder and nutrient-rich intermediate and deep waters to the mixed layer. It is during these productive events, mainly during winter–spring transition, when the highest annual coccolithophore production occurs (Rigual-Hernández et al., 2013). Coccolithophores are one of the main producers of C_{37} – C_{39} long-chain ketones with two to four double bonds, known as alkenones (e.g., Volkman et al., 1980). The relative content of unsaturated ketones depends on the growth temperature of the microalgae (Brassell et al., 1986) and thus the alkenone ratio in sediments can be used for reconstructing past SSTs. Therefore, the SST estimates inferred from this indicator in the Gulf of Lions can be used to reconstruct the SSTs during the periods of maximum production and export of coccolithophores, i.e. the annual upwelling events during the winter–spring transition.

3. Methods

A total of 197 samples (1 cm thick slices) for biomarker analysis were taken from borehole PRGL1 between 231.44 mbsf (440 kyr) to 300.58 mbsf (528 kyr), covering MIS 12 to MIS 13. In order to avoid significant differences in the age resolution due to differences in the sedimentation rates during glacial and interglacial periods (Sierro et al., 2009), samples were taken every 20 cm during glacials and 1 cm during interglacials. The estimated alkenone-based SST reconstructions for MIS 12 and MIS 13 are plotted in Fig. 2b (red line). Moreover, the four climate cycles following MIS 12 (from 29–440 kyr) (Cortina et al., 2015) are also shown in Fig. 2b (orange line) (data available online: <http://doi.pangaea.de/10.1594/PANGAEA.854682>) in order to compare MIS 13 with other interglacials. Furthermore, data for the terrestrial derived bottom oxygenation index (898 samples) are also provided for the first time covering the last five climate cycles (23–528 kyr) (Fig. 2c).

3.1. Age model

From 19 to 157.10 mbsf, we used the age model published by Sierro et al. (2009). For the second interval (from 157.10 to 300.58 mbsf) we used the age model published by Frigola et al. (2012). In both cases the age model was mainly based on comparison of the *Globigerina bulloides* $\delta^{18}O$ record with the LR04 benthic stack (Lisiecki and Raymo, 2005) with the exception of the upper part where the isotope record was tuned to Greenland ice cores. Including all sources of error, the uncertainty in the LR04 age model has been estimated to be 4 kyr from 1000 kyr to present (Lisiecki and Raymo, 2005).

The calculated sedimentation rates resulted in an average sampling resolution of 1150 yr during interglacials and 160 yr during glacial stages. The base of PRGL1 was deduced to correspond to MIS 13 taking into consideration the sedimentary units identified and the extinction of the coccolithophore *Pseudoemiliania lacunosa* at about 275 m (Frigola et al., 2012).

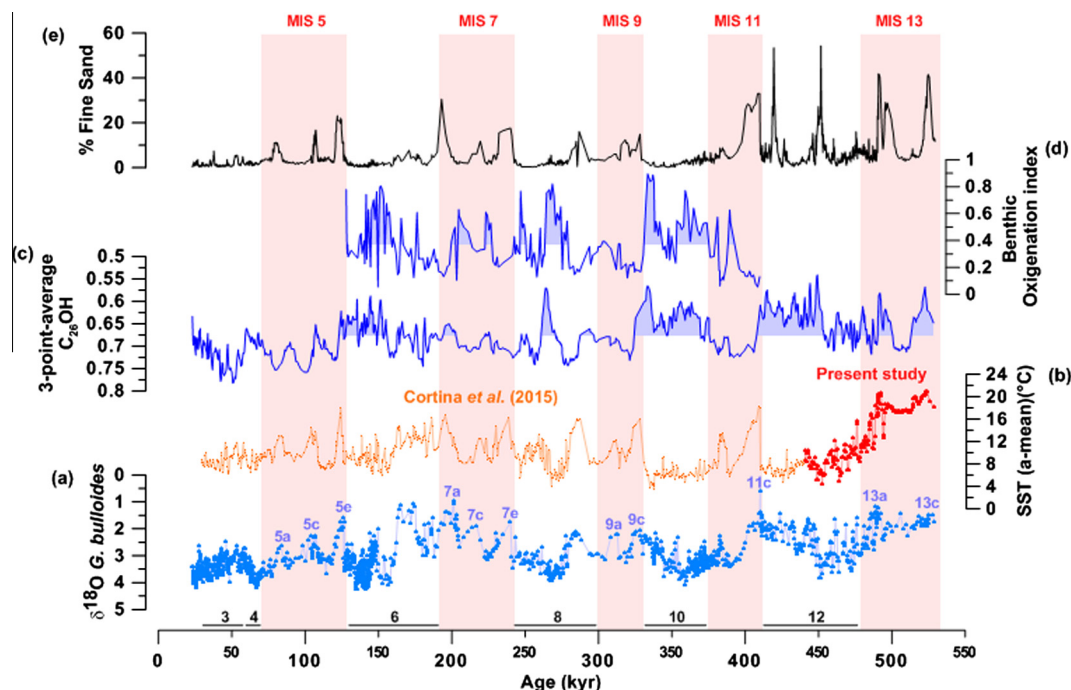


Fig. 2. SST and oxygenation of the bottom waters variability in the Gulf of Lions from MIS 3 to MIS 13. (a) *G. bulloides* $\delta^{18}\text{O}$ values. The values from 29–265 kyr were taken from Sierro et al. (2009), while values from 266–528 kyr were taken from Frigola et al. (2012). (b) SST alkenone-derived profile from MIS 3 to MIS 13. Values from 29–440 kyr (orange) were taken from Cortina et al. (2015). In this study we present new SST values from 440–528 kyr (red). (c) 3-point-average C_{26}OH index. The values are represented in inverse order; i.e. lower values indicate higher bottom oxygenation events. (d) Benthic Oxygenation Index (Cortina et al., 2013) from MIS 6 to MIS 11. (e) % fine sand (<63 μm) (Sierro et al., 2009). Orange bars mark interglacial stages. (For interpretation of the references to color in this figure legend, the reader is referred to the web version of this article.)

3.2. Biomarker sediment extraction

Samples were freeze-dried. Biomarker extraction was based on the procedure of Villanueva et al. (1997). We added an internal standard (*n*-nonadecan-1-ol, *n*-hexatriacontane and *n*-dotetracontane) to about 2.5 g of sediment that was extracted with dichloromethane in an ultrasonic bath. The extract was saponified with 10% KOH in methanol to clean up the interferences with carboxylic acids and wax esters. The phase with the neutral lipids was extracted with hexane which was evaporated to dryness under N_2 . Finally, the compounds were re-dissolved using toluene and derivatized with bis(tri methylsilyl)trifluoroacetamide and analyzed by gas chromatography. The samples were analyzed with a Varian 3400 equipped with a CPSIL-5 CB column coated with 100% dimethylsiloxane (film thickness 0.12 mm). Hydrogen was the carrier gas (50 cm/s). The oven was programmed from 90–170 °C at 20 °C/min, then to 280 °C at 6 °C/min (hold time 35 min), to 300 °C at 10 °C/min (hold time 7 min) and finally to 320 °C at 10 °C/min (hold time 3 min). The injector was programmed from 90 °C (hold time 0.3 min) to 320 °C at 200 °C/min (final hold time was 20 min). The detector was maintained at 320 °C.

From chromatograms, *n*-nonacosane, *n*-hexacosanol and long chain di- and tri- unsaturated C_{37} alkenones were identified. The areas under the peaks were then integrated and the resulting values converted to concentrations taking into consideration sample weight and internal standard concentration. For this protocol, absolute concentration errors were < 10% and reproducibility tests showed that the uncertainty in the U_{37}^K determinations were less than 0.015 (ca. ± 0.5 °C) (Martrat et al., 2003).

The SST proxy was based on the U_{37}^K index (Brassell et al., 1986; Prahl and Wakeham, 1987). The U_{37}^K index results from calculating the relative abundance of alkenones, both with 37 carbons but differing number of double bonds.

$$U_{37}^K = [\text{C}_{37:2}]/([\text{C}_{37:2}] + [\text{C}_{37:3}]);$$

This index can have values between 0 and 1 which corresponds to temperatures between 0 and 29 °C respectively. To transform this index into annual mean SST values we utilized the equation:

$$\text{SST} = (U_{37}^K - 0.044)/0.033 \quad (\text{Müller et al., 1998}).$$

We used the C_{26}OH index (i.e. *n*-hexacosanol/(*n*-nonacosane + *n*-hexacosanol)) as a proxy of bottom ventilation. The C_{26}OH index (Cacho et al., 2000; Martrat et al., 2007) is a chemical proxy that reflects bottom oxygenation, since both compounds have the same origin but different susceptibility to degradation. The C_{26}OH index decreases with increasing bottom water oxygenation.

4. Results

4.1. Sea surface temperature (SST)

Broadly, the SST profile follows the *G. bulloides* $\delta^{18}\text{O}$ record (Fig. 2a and b). Table 1 summarizes the SST statistics from MIS 3 to MIS 13: average, minimum, maximum and standard deviation. The average SST during MIS 12 was 8.1 °C (standard deviation: 1.9) with a maximum value of 15.8 °C and a minimum of 4.3 °C (Fig. 2b). When compared with the following glacials this was the second coldest glacial after MIS 10. Moreover, its SST profile showed a strong millennial variability (Fig. 2b). Meanwhile, in the Gulf of Lions, the MIS 13 was the warmest interglacial of the last 530 kyr. The average SST was 16.9 °C and exceeded by more than 5 °C the second warmest interglacial (i.e. MIS 7: 11.1 °C). The maximum value was 21.1 °C, which is 2.9 °C greater than the second maximum reached at MIS 11 (18.2 °C). Unlike the rest of interglacials analyzed, MIS 13 did not record strong differences between warmer and colder sub-stages (Fig. 2b).

Table 1

SST statistical parameters from MIS 3 to MIS 13. Values from 29–440 kyr were taken from Cortina et al. (2015). In this study we present new SST values from 440–528 kyr.

MIS	SST average	SST maximum	SST minimum	Standard deviation	Source
3–4	8.7	11.7	6.3	1.3	Cortina et al. (2015)
5	10.1	18.1	6.9	2.4	Cortina et al. (2015)
6	10.2	16.1	5.8	2.3	Cortina et al. (2015)
7	11.1	16.6	8.1	2.2	Cortina et al. (2015)
8	9.3	16.0	4	2.8	Cortina et al. (2015)
9	10.8	16.0	7.2	2.2	Cortina et al. (2015)
10	6.1	9.2	3.5	1.1	Cortina et al. (2015)
11	10.9	18.2	5.8	3.3	Cortina et al. (2015)
12	8.1	15.8	4.3	1.9	Cortina et al. (2015)
13	16.9	21.1	10.1	3	Present study Present study

4.2. Bottom oxygenation

The $C_{26}OH$ index showed minimum values (implying maximum ventilation of bottom sediments) during glacial stages, specifically during MIS 6, 10 and 12 (Fig. 2c). Although one of the strongest oxygenation events occurred during MIS 8, the $C_{26}OH$ index remained high at the end of this stage. During interglacial stages, oxygenation remained low punctuated by some oxygenation events during glacial sub-stages (e.g., 5b, 5d). However, this general glacial-interglacial pattern was interrupted during MIS 13. During this period oxygenation achieved values similar to those of glacial periods. Moreover, higher oxygenation values were reached during interglacial sub-stages (e.g., 13c, 13a) decreasing at times of glacial sub-stage 13b.

5. Discussion

5.1. The reliability of the $C_{26}OH$ index as indicator of bottom sediment oxygenation

The $C_{26}OH$ index could be influenced by the glacial/interglacial differential sedimentation rates occurring at the upper slope of the Gulf of Lions reducing its reliability as a bottom sediment oxygenation index. During glacial stages a drop in sea level led to the accumulation of large amounts of sediment from the Rhône on the upper slope causing a rapid organic matter burial. In contrast, during interglacial stages sediment input decreased as a consequence of landward migration of the Rhône river mouth (Sierra et al., 2009). Due to this decrease, the organic matter remained longer under the influence of bottom waters. Such differences in the time that organic matter remains exposed to bottom waters might produce a differential degradation of the organic compounds causing variations of the $C_{26}OH$ index owing to river input rather than oceanographic processes.

However, the agreement between the bottom oxygenation index (Cortina et al., 2013) (Fig. 2d), calculated from benthic foraminifer assemblages, and the $C_{26}OH$ index (Fig. 2c) from MIS 6 to MIS 11, allows us to consider the $C_{26}OH$ index as a reliable indicator of bottom oxygenation. Although sedimentation rates could play a role in the $C_{26}OH$ index variability, this effect was overcome by strong glacial/interglacial bottom oxygenation differences.

5.2. SST response to atmospheric variability at the Gulf of Lions

The dating of the bottom of borehole PRGL1 presents a certain degree of uncertainty. Both the comparison of the *G. bulloides* $\delta^{18}O$ record with the LR04 benthic stack (Lisiecki and Raymo, 2005) and the evidence argued by Frigola et al. (2012) place the bottom of the drill at MIS 13. In this study, further evidence will be added that is consistent with the latter studies indicating that the bottom of the core corresponds to the base of the MIS 13. During high sea levels, when the coastline was distant from the upper slope, the pro-deltaic and coastal sediments supplied by the Rhône were accommodated in the continental shelf. This situation resulted in low sedimentation rates with the deposition of mainly biogenic material on the upper slope of the Gulf of Lions. Through the analysis of the contribution of fine sand ($>63 \mu m$) in PRGL1, Sierra et al. (2009) identified these biogenic-rich layers associated with high stands and named them Condensed Layers (CL's). During MIS 5 and MIS 7, all these layers were precisely associated with interglacial sub-stages (MIS 5a, 5c, 5d, 7a, 7c and 7d) owing to an associated sea level increase. This pattern is repeated throughout PRGL1 (Fig. 2e) and at times of MIS 13, two main CL's were formed that were most probably linked to MIS 13a and 13c. All the above lead us to conclude that the base of the drill corresponds to MIS 13c.

In terms of SSTs, MIS 13 represents the warmest interglacial of the last 530 kyr. In contrast to the following interglacials, no strong glacial-interglacial sub-stage SST gradient was found. These warm conditions are in contrast with several other registers, mainly in southern locations (Becquey and Gersonde, 2002; Lisiecki and Raymo, 2005; Jouzel et al., 2007; Voelker et al., 2010). The evidence that supports the idea of a cooler MIS 13 compared with younger interglacials are: (1) high oxygen isotope values that are broadly interpreted as a signal of larger ice content (Lisiecki and Raymo, 2005) (Fig. 3c); (2) according to EDC δD (Fig. 3d) it is the coolest interglacial of the last 800 kyr (Jouzel et al., 2007); (3) Summer sea surface temperature (SSST) in the sub-Antarctic Atlantic was the lowest among interglacials of the past 550 kyr (Becquey and Gersonde, 2002); (4) SST records from the mid-latitude Atlantic reveal MIS 13 as colder than younger interglacials (Voelker et al., 2010).

In contrast, northern terrestrial records are in agreement with the hypothesis of a warmer MIS 13 interglacial than monitored in the south (Chen et al., 1999; Vandenberghe, 2000; Prokopenko et al., 2002; Sun et al., 2006; de Vernal and Hillaire-Marcel, 2008; Marković et al., 2009; Guo et al., 2009; Fitzsimmons et al., 2012). The China Loess record, covering the last 800 kyr, revealed an extremely weak winter monsoon during MIS 13 (Fig. 3b) together with the lowest inland aridity and extreme summer monsoon (Guo et al., 2009). Geological records (Ding et al., 1995; Porter and An, 1995; Guo et al., 2004) or climate models (Ruddiman and Kutzbach, 1989; Wu and Wang, 2002) indicated a close link between the Asian winter monsoon and ice conditions in the northern high-latitudes, with a weakened Asian winter monsoon at times of low ice volume. The MIS 13–15 Loess deposits of the middle and lower Danube River basin, from Hungary eastward, in southeastern Europe (Fitzsimmons et al., 2012) monitored relatively humid conditions with mild and humid winters and hot summers and autumns. This deposit is the most strongly developed and corresponds to the most humid conditions of the most recent 16 isotope stages (Marković et al., 2009).

Besides Loess deposits, studies carried out in lake sediments in the Northern Hemisphere also showed that MIS 13 was a full interglacial without a cool imprint as registered in the Southern Hemisphere. Chen et al. (1999) identified MIS 13 as the warmest interglacial over the last 800 kyr in the eastern Tibetan Plateau. Sediment record from Lake Baikal, Siberia (Prokopenko et al., 2002)

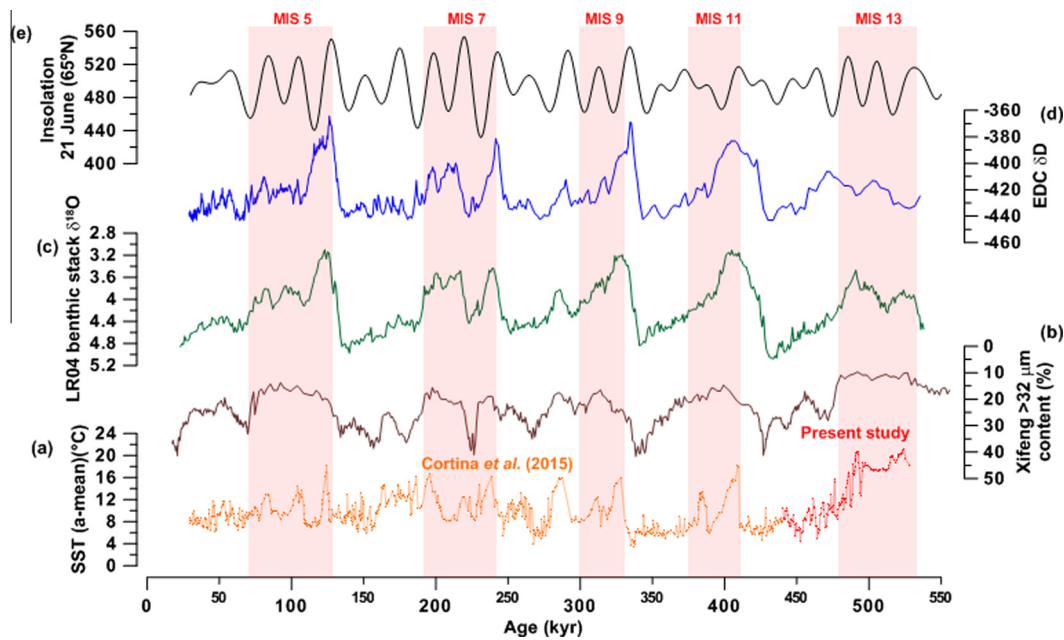


Fig. 3. Northern and southern climate records for the last 530 kyr. (a) SST alkenone-derived profile from MIS 3 to MIS 13. Values from 29–440 kyr (orange) were taken from Cortina et al. (2015). In this study we present new SST values from 440–528 kyr (red). (b) Loess grain-size changes shown by the content > 32 μm fraction at Xifeng (Guo et al., 2009). Low values are linked to weakened Asian winter monsoon. (c) LR04 benthic stack $\delta^{18}\text{O}$ (Lisiecki and Raymo, 2005). (d) Antarctic temperature as reflected by the EDC δD record (Jouzel et al., 2007). (e) Insolation at 21 of June (65°N) (Laskar et al., 2004). Orange bars mark interglacial stages. (For interpretation of the references to color in this figure legend, the reader is referred to the web version of this article.)

reveal a virtually continuous interglacial diatom assemblage and lithogenic sediments with “interglacial” characteristics for the period from MIS 11 to MIS 15a, inferring an apparent lack of extensive mountain glaciation. All the above evidence lead us to conclude that MIS 13 was characterized by a strong asymmetry of hemispheric climates with average cooler conditions in the Southern Hemisphere and generally warmer conditions in the Northern Hemisphere (Guo et al., 2009). Hence, regarding ice volume, we should expect a strong asymmetry between the two hemispheres. Guo et al. (2009) based this assumption on the fact that although marine $\delta^{18}\text{O}$ benthic records had a strong signal of global ice volume (Lisiecki and Raymo, 2005), it does not discriminate between northern and southern ice-sheet signals. Moreover, substantially reduced Greenland ice volume characterized MIS 13 (de Vernal and Hillaire-Marcel, 2008). In contrast, Ziegler et al. (2010), based on primary productivity records on the north-eastern Arabian Sea, linked the high productivity levels recorded during MIS 13 with an enhancement of the Atlantic Overturning Circulation (Raymo et al., 1997) that might have triggered mild winters found in large parts of Northern Hemisphere that in turn weakened Asian winter monsoons. They discarded an odd monsoon event proposed by previous studies on the basis of low insolation (Laskar et al., 2004), low methane records from Antarctic ice cores (Louergue et al., 2008) and low isotope benthic profile (Lisiecki and Raymo, 2005).

It has been demonstrated that the strong influence of continental climate via cold north-westerly winds in the northwestern Mediterranean Sea (Cacho et al., 2000; Kuhlemann et al., 2008) and specifically in the SST of the upper slope of the Gulf of Lions (Cortina et al., 2015). As insolation alone cannot account for the increase of SST in the area during MIS 13 (Fig. 3a and e), this anomalous rise should be the result of changes in atmospheric conditions.

Present climate dynamics in the Mediterranean Basin are highly influenced by seasonal ITCZ shifts. During summer, the establishment of a stable high-pressure system characterizes the Mediterranean resulting in hot and dry conditions (Fig. 4b). In contrast, during the winter months, the southward migration of the

high-pressure system results in cooler and wetter weather (Fig. 4a) (Cramp and O’Sullivan, 1999). During these periods, there is an enhancement of the channeled cold winds passing through the Pyrenees passages in the Gulf of Lions causing a drop in the SST values. Today, the ITCZ penetrates into the Northern Hemisphere in summer as far as 24°N . Nonetheless, changes in its summer position at interglacial/glacial timescales have been reported from both insolation (Chiang et al., 2003; Stoll et al., 2007; Tzedakis, 2010) and ice-sheet volume (Chiang and Bitz, 2005) changes. The summer ITCZ position migrated further north during periods with high insolation and low northern ice volume and vice versa. A more northward position in winter than today could prevent the entrance of cool north-westerly winds inhibiting the cooling effect on the sea surface. As stated before, owing to its low values, the hypothesis that insolation triggers the displacement of the northern ITCZ can be rejected. However, the asymmetrical distribution of ice sheets proposed by Guo et al. (2009) seems to be in agreement with our results. A global scenario with ice volume accommodated preferably in southern locations might result in a more northward position of the ITCZ during both summer and winter. This atmospheric configuration would prevent the entrance of cool north-westerly winds during the whole or most of the year. The result would be a SST profile with warmer values during MIS 13 than the younger interglacials, as recorded in the Gulf of Lions.

5.3. Enhancement of bottom ventilation events during MIS 13 interglacial sub-stages

The northward position of the ITCZ during MIS 13 both in summer and winter would produce a new atmospheric pattern over the Gulf of Lions. Western Mediterranean Deep Water (WMDW) formation takes place in the Gulf of Lions, and cold north-westerly winds play an important role in this process (Cacho et al., 2000). The rate of WMDW formation determines the strength of the Mediterranean thermohaline circulation and the exchange with Atlantic waters through the Strait of Gibraltar. Therefore, changes in the atmospheric patterns over the Gulf of Lions could

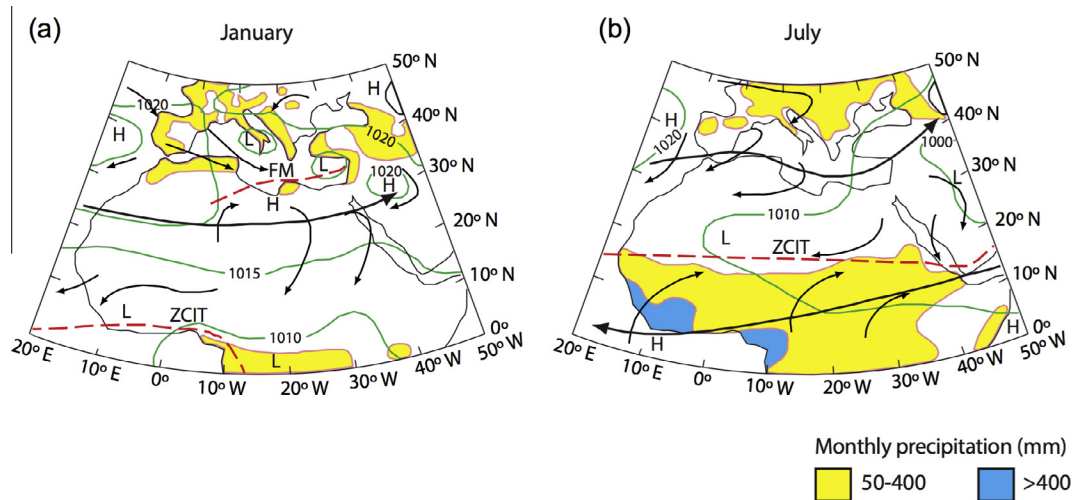


Fig. 4. Map showing the distribution of surface pressure, winds and precipitation levels for the Mediterranean and North Africa during (a) winter (January) and (b) summer (July). The average position of the Subtropical and Easterly Jet Streams is represented with arrows. Abbreviations: Inter Tropical Convergence Zone – ITCZ, Mediterranean Front – MF, areas of high pressure – H, areas of low pressure – L. Figure adapted from Cramp and O’Sullivan (1999).

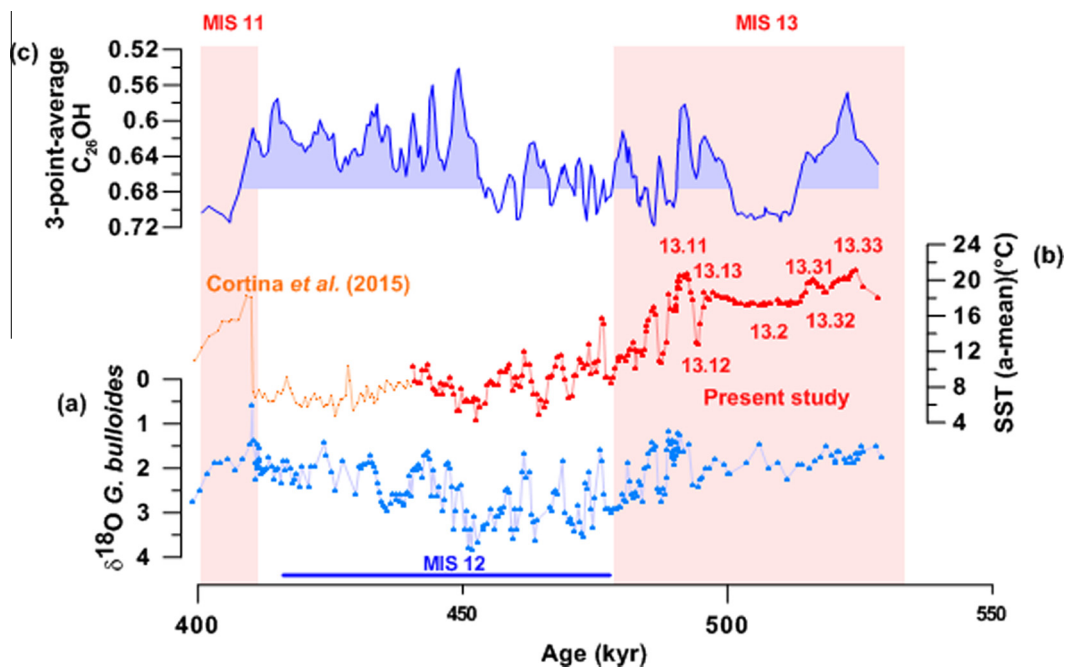


Fig. 5. High-resolution SST and oxygenation of the bottom waters profiles in the Gulf of Lions during MIS 12 and 13. (a) *G. bulloides* $\delta^{18}\text{O}$ values (Frigola et al., 2012). (b) SST alkenone-derived profile. Values from 400–440 kyr (orange) were taken from Cortina et al. (2015). In this study we present new SST values from 440–528 kyr (red) (c) 3-point-average C_{26}OH index. The values are represented in inverse order; i.e. lower values indicate higher bottom oxygenation events. Orange bars mark interglacial stages. (For interpretation of the references to color in this figure legend, the reader is referred to the web version of this article.)

induce changes in WMDW formation affecting the entire Mediterranean basin through the exchange of heat and salt with the Atlantic.

Although WMDW formation does not take place at the location of PRGL1, our core site is in the path of north-westerly winds and registered an increase in their intensity from MIS 6 to MIS 11 during cold episodes as suggested by the appearance of benthic foraminifer adapted to oxygenated bottom conditions (Cortina et al., 2011, 2013). Moreover, these observations are consistent with previous studies in the northwestern Mediterranean that documented an increase of WMDW during last glacial stadial events (Cacho et al., 2000; Sierro et al., 2005). Taken together, our data and these

regionally relevant studies strongly suggest that the increase of north-westerly winds during cold periods enhanced water mixing at the upper slope bringing oxygenated waters to the bottom. At the same time, a highly probable intensification of WMDW formation should be monitored at its source area.

The increase of bottom oxygenation during cold periods is monitored from MIS 2 to MIS 12 with the only exception being an interval centered on 265 kyr (MIS 8) (Fig. 2c). During this interval, an increase of arboreal pollen at Tenaghi Philippon has been reported (Tzedakis et al., 2003). In addition, SST reconstruction (Fig. 2b) and benthic foraminifer adapted to mesotrophic conditions at PRGL1 are indicative of a sea level increase (Cortina et al., 2013). All these

data suggest that, although MIS 8 was a glacial stage, the interval centered about 265 kyr exhibited relatively warm conditions with associated bottom oxygenation weakening.

Despite the fact that the cold stages were generally associated with an intensification of bottom oxygenation, our data suggests that MIS 13 followed an opposite trend with enhancement of the bottom oxygenation during warmer periods (e.g., 13.11, 13.13, 13.31 and 13.33) (Fig. 5b and c) and a weakening during colder periods (e.g., 13.12, 13.2 and 13.32). After the 13.11 event, millennial glacial enhancement found in previous studies (Cacho et al., 2000; Sierro et al., 2005; Cortina et al., 2011, 2013) was observed (Fig. 5b and c).

We hypothesize that the blocking effect on passages owing to a more northward position of the ITCZ position in winter, together with low north ice volume, could stop the stadial reinforcement of north-westerly winds. Nonetheless, after the 13.11 event, the northern ice sheet reached a critical volume that caused a southward displacement of the ITCZ, allowing the entrance of north-westerly winds in winter and promoting their glacial sub-stage enhancement (Cacho et al., 2000; Sierro et al., 2005; Cortina et al., 2011, 2013).

What remains unclear is the mechanism that boosted bottom ventilation during the warmer stages of MIS 13. Two possible mechanisms could explain this behavior. First, the new atmospheric configuration enhanced the entrance of southern winds during warmer stages producing an increased mixing of the water column bringing oxygenated waters to the bottom. Second, a reinforcement of the North Current flowing through the upper slope during warmer stages would oxygenate bottom waters. Further research is necessary to unveil the ultimate mechanism that triggered a reinforcement of bottom oxygenation during warmer sub-stages of MIS 13 that differed from the following interglacials.

6. Conclusions

During MIS 13, northern and southern paleoclimate records seem to be in disagreement. While southern paleorecords monitored an interglacial cooler than younger interglacials, northern continental paleo-data seem to support an interglacial with similar or even warmer conditions than those that followed it. Our long and high-resolution SST record in the Gulf of Lions shows that it was highly influenced by continental conditions and reflected a warmer MIS 13 compared with the younger interglacials. We suggest that due to the decrease of northern ice volume and its accumulation in the southern hemisphere both the summer and winter ITCZ positions migrated northward preventing the entrance of the cool channeled north-westerly winds during winter. The result was a MIS 13 warmer than the following interglacials in which north-westerly winds cooled western Mediterranean waters mainly in winter. The different atmospheric pattern created by northward displacement of ITCZ promoted the oxygenation of the bottom waters in the upper slope during warmer stages, contrary to the stadial reinforcement recorded in late Quaternary paleorecords. The main causes of these “warm” bottom oxygenation enhancements remain unclear and could be as a consequence of either a North Current intensification or a reinforcement of the southerly winds.

Acknowledgments

Two anonymous reviewers are greatly acknowledged for their comments that improved the final version of this manuscript. J.K. Volkman and B.E. van Dongen are also acknowledged for their suggestions. This work was funded by the Spanish “Ministerio de Ciencia e Innovación” MICINN project CGL2011-26493 and GRACCIE

(CONSOLIDER-INGENIO CSD 2007-00067) and the Regional Government of Castilla y León Project GR34.

Appendix A. Supplementary data

Supplementary data associated with this article can be found, in the online version, at <http://dx.doi.org/10.1016/j.orggeochem.2015.12.004>.

Associate Editor—Bart van Dongen

References

- Aloisi, J.C., 1986. Sur un modèle de sédimentation deltaïque: contribution à la connaissance des marges passives. Université de Perpignan, Perpignan, 162 p.
- Becquey, S., Gersonde, R., 2002. Past hydrographic and climatic changes in the Subantarctic Zone of the South Atlantic – The Pleistocene record from ODP Site 1090. *Palaeogeography, Palaeoclimatology, Palaeoecology* 182, 221–239.
- Béthoux, J.P., 1984. Paleoclimatographic changes in the Mediterranean Sea in the last 20,000 years. *Oceanologica Acta* 7, 43–48.
- Brassell, S.C., Eglinton, G., Marlowe, I.T., Pflaumann, U., Sarnthein, M., 1986. Molecular stratigraphy: a new tool for climatic assessment. *Nature* 320, 129–133.
- Cacho, I., Grimalt, J.O., Sierro, F.J., Shackleton, N., Canals, M., 2000. Evidence for enhanced Mediterranean thermohaline circulation during rapid climatic coolings. *Earth and Planetary Science Letters* 183, 417–429.
- Chen, F.H., Bloemendal, J., Zhang, P.Z., Liu, G.X., 1999. An 800 kyr proxy record of climate from lake sediments of the Zoige Basin, eastern Tibetan Plateau. *Palaeogeography, Palaeoclimatology, Palaeoecology* 151, 307–320.
- Chiang, J.H., Bitz, C., 2005. Influence of high latitude ice cover on the marine Intertropical Convergence Zone. *Climate Dynamics* 25, 477–496.
- Chiang, J.C.H., Biasutti, M., Battisti, D.S., 2003. Sensitivity of the Atlantic Intertropical Convergence Zone to Last Glacial Maximum boundary conditions. *Palaeogeography* 18, 1094.
- Cortina, A., Sierro, F.J., González-Mora, B., Asioli, A., Flores, J.A., 2011. Impact of climate and sea level changes on the ventilation of intermediate water and benthic foraminifer assemblages in the Gulf of Lions, off South France, during MIS 6 and 7. *Palaeogeography, Palaeoclimatology, Palaeoecology* 309, 215–228.
- Cortina, A., Sierro, F.J., Filippelli, G., Flores, J.A., Berné, S., 2013. Changes in planktic and benthic foraminifer assemblages in the Gulf of Lions, off south France: response to climate and sea level change from MIS 6 to MIS 11. *Geochemistry, Geophysics, Geosystems* 14, 1258–1276.
- Cortina, A., Sierro, F.J., Flores, J.A., Martrat, B., Grimalt, J.O., 2015. The response of SST to insolation and ice sheet variability from MIS 3 to MIS 11 in the northwestern Mediterranean Sea (Gulf of Lions). *Geophysical Research Letters* 42. <http://dx.doi.org/10.1002/2015GL065539>.
- Cramp, A., O’Sullivan, G., 1999. Neogene sapropels in the Mediterranean: a review. *Marine Geology* 153, 11–28.
- de Vernal, A., Hillaire-Marcel, C., 2008. Natural variability of Greenland climate, vegetation, and ice volume during the past million years. *Science* 320, 1622–1625.
- Ding, Z., Liu, T., Rutter, N.W., Yu, Z., Guo, Z., Zhu, R., 1995. Ice-volume forcing of East Asian winter monsoon variations in the past 800,000 years. *Quaternary Research* 44, 149–159.
- Fitzsimmons, K.E., Marković, S.B., Hambach, U., 2012. Pleistocene environmental dynamics recorded in the loess of the middle and lower Danube basin. *Quaternary Science Reviews* 41, 104–118.
- Frigola, J., Canals, M., Cacho, I., Moreno, A., Sierro, F.J., Flores, J.A., Berné, S., Jouet, G., Dennielou, B., Herrera, G., Pasqual, C., Grimalt, J.O., Galavazi, M., Schneider, R., 2012. A 500 kyr record of global sea-level oscillations in the Gulf of Lion, Mediterranean Sea: new insights into MIS 3 sea-level variability. *Climate of the Past* 8, 1067–1077.
- Guo, Z., Peng, S., Hao, Q., Biscaye, P.E., An, Z., Liu, T., 2004. Late Miocene-Pliocene development of Asian aridification as recorded in the Red-Earth Formation in northern China. *Global and Planetary Change* 41, 135–145.
- Guo, Z.T., Berger, A., Yin, Q.Z., Qin, L., 2009. Strong asymmetry of hemispheric climates during MIS-13 inferred from correlating China loess and Antarctica ice records. *Climate of the Past* 5, 21–31.
- Jouet, G., Berné, S., Rabineau, M., Bassetti, M.A., Bernier, P., Dennielou, B., Sierro, F.J., Flores, J.A., Taviani, M., 2006. Shoreface migrations at the shelf edge and sea-level changes around the Last Glacial Maximum (Gulf of Lions, NW Mediterranean). *Marine Geology* 234, 21–42.
- Jouzel, J., Masson-Delmotte, V., Cattani, O., Dreyfus, G., Falourd, S., Hoffmann, G., Minster, B., Nouet, J., Barnola, J.M., Chappellaz, J., Fischer, H., Gallet, J.C., Johnsen, S., Leuenberger, M., Loulergue, L., Luethi, D., Oerter, H., Parrenin, F., Raisbeck, G., Raynaud, D., Schilt, A., Schwander, J., Selmo, E., Souchez, R., Spahni, R., Stauffer, B., Steffensen, J.P., Stenni, B., Stocker, T.F., Tison, J.L., Werner, M., Wolff, E.W., 2007. Orbital and millennial Antarctic climate variability over the past 800,000 years. *Science* 317, 793–796.
- Kuhlemann, J., Rohling, E.J., Krumrei, I., Kubik, P., Ivy-Ochs, S., Kucera, M., 2008. Regional synthesis of Mediterranean atmospheric circulation during the Last Glacial Maximum. *Science* 321, 1338–1340.

- Laskar, J., Robutel, P., Joutel, F., Gastineau, M., Correia, A.C.M., Levrard, B., 2004. A long-term numerical solution for the insolation quantities of the Earth. *Astronomy and Astrophysics* 428, 261–285.
- Lisiecki, L.E., Raymo, M.E., 2005. A Pliocene–Pleistocene stack of 57 globally distributed benthic $\delta^{18}\text{O}$ records. *Paleoceanography* 20, PA1003.
- Loulergue, L., Schilt, A., Spahni, R., Masson-Delmotte, V., Blunier, T., Lemieux, B., Barnola, J.-M., Raynaud, D., Stocker, T.F., Chappellaz, J., 2008. Orbital and millennial-scale features of atmospheric CH_4 over the past 800,000 years. *Nature* 453, 383–386.
- Marković, S.B., Hambach, U., Catto, N., Jovanović, M., Buggle, B., Machalet, B., Zöller, L., Glaser, B., Frechen, M., 2009. Middle and Late Pleistocene loess sequences at Batajnica, Vojvodina, Serbia. *Quaternary International* 198, 255–266.
- Martrat, B., Grimalt, J.O., Villanueva, J., van Kreveld, S., Sarnthein, M., 2003. Climatic dependence of the organic matter contributions in the north eastern Norwegian Sea over the last 15,000 years. *Organic Geochemistry* 34, 1057–1070.
- Martrat, B., Grimalt, J.O., Shackleton, N.J., de Abreu, L., Hutterli, M.A., Stocker, T.F., 2007. Four climate cycles of recurring deep and surface water destabilizations on the Iberian Margin. *Science* 317, 502–507.
- Millot, C., 1982. Analysis of Upwelling in the Gulf of Lions. Elsevier, Elsevier Oceanography Series, pp. 143–153.
- Millot, C., 1990. The Gulf of Lions' hydrodynamics. *Continental Shelf Research* 10, 885–894.
- Müller, P.J., Kirst, G., Ruhland, G., von Storch, J., Rosell-Melé, A., 1998. Calibration of the alkenone paleotemperature index U_{37}^K based on core-tops from the eastern South Atlantic and the global ocean (60°N–60°S). *Geochimica et Cosmochimica Acta* 62, 1757–1772.
- Pflaumann, U., Sarnthein, M., Chapman, M., d'Abreu, L., Funnell, B., Huels, M., Kiefer, T., Maslin, M., Schulz, H., Swallow, J., van Kreveld, S., Vautravers, M., Vogelsang, E., Weinelt, M., 2003. Glacial North Atlantic: sea-surface conditions reconstructed by GLAMAP 2000. *Paleoceanography* 18, 1065.
- Porter, S.C., An, Z.S., 1995. Correlation between climate events in the North Atlantic and China during the last glaciation. *Nature* 375, 305–308.
- Prahl, F.G., Wakeham, S.G., 1987. Calibration of unsaturation patterns in long-chain ketone compositions for palaeotemperature assessment. *Nature* 330, 367–369.
- Prokopenko, A.A., Williams, D.F., Kuzmin, M.I., Karabanov, E.B., Khursevich, G.K., Peck, J.A., 2002. Muted climate variations in continental Siberia during the mid-Pleistocene epoch. *Nature* 418, 65–68.
- Rabineau, M., Berné, S., Aslanian, D., Olivet, J.L., Joseph, P., Guillocheau, F., Bourillet, J.F., Ledrezen, E., Granjeon, D., 2005. Sedimentary sequences in the Gulf of Lion: a record of 100,000 years climatic cycles. *Marine and Petroleum Geology* 22, 775–804.
- Raymo, M.E., Oppo, D.W., Curry, W., 1997. The Mid-Pleistocene climate transition: a deep sea carbon isotopic perspective. *Paleoceanography* 12, 546–559.
- Rigual-Hernández, A.S., Bárcena, M.A., Jordan, R.W., Sierro, F.J., Flores, J.A., Meier, K.J. S., Beaufort, L., Heussner, S., 2013. Diatom fluxes in the NW Mediterranean: evidence from a 12-year sediment trap record and surficial sediments. *Journal of Plankton Research* 35, 1109–1125.
- Ruddiman, W.F., Kutzbach, J.E., 1989. Forcing of late Cenozoic northern hemisphere climate by plateau uplift in southern Asia and the American west. *Journal of Geophysical Research: Atmospheres* 94, 18409–18427.
- Sierro, F.J., Hodell, D.A., Curtis, J.H., Flores, J.A., Reguera, I., Colmenero-Hidalgo, E., Bárcena, M.A., Grimalt, J.O., Cacho, I., Frigola, J., Canals, M., 2005. Impact of iceberg melting on Mediterranean thermohaline circulation during Heinrich events. *Paleoceanography* 20, PA2019.
- Sierro, F.J., Andersen, N., Bassetti, M.A., Berne, S., Canals, M., Curtis, J.H., Dennielou, B., Flores, J.A., Frigola, J., Gonzalez-Mora, B., Grimalt, J.O., Hodell, D.A., Jouet, G., Perez-Folgado, M., Schneider, R., 2009. Phase relationship between sea level and abrupt climate change. *Quaternary Science Reviews* 28, 2867–2881.
- Stoll, H.M., Vance, D., Arealos, A., 2007. Records of the Nd isotope composition of seawater from the Bay of Bengal: implications for the impact of Northern Hemisphere cooling on ITCZ movement. *Earth and Planetary Science Letters* 255, 213–228.
- Sun, Y., Clemens, S.C., An, Z., Yu, Z., 2006. Astronomical timescale and palaeoclimatic implication of stacked 3.6-Myr monsoon records from the Chinese Loess Plateau. *Quaternary Science Reviews* 25, 33–48.
- Tzedakis, P.C., 2010. The MIS 11–MIS 1 analogy, southern European vegetation, atmospheric methane and the “early anthropogenic hypothesis”. *Climate of the Past* 6, 131–144.
- Tzedakis, P.C., McManus, J.F., Hooghiemstra, H., Oppo, D.W., Wijmstra, T.A., 2003. Comparison of changes in vegetation in northeast Greece with records of climate variability on orbital and suborbital frequencies over the last 450,000 years. *Earth and Planetary Science Letters* 212, 197–212.
- Vandenbergh, J., 2000. A global perspective of the European chronostratigraphy for the past 650 ka. *Quaternary Science Reviews* 19, 1701–1707.
- Villanueva, J., Pelejero, C., Grimalt, J.O., 1997. Clean-up procedures for the unbiased estimation of C_{37} alkenone sea surface temperatures and terrigenous *n*-alkane inputs in paleoceanography. *Journal of Chromatography A* 757, 145–151.
- Voelker, A.H.L., Rodrigues, T., Billups, K., Oppo, D., McManus, J., Stein, R., Hefter, J., Grimalt, J.O., 2010. Variations in mid-latitude North Atlantic surface water properties during the mid-Brunhes (MIS 9–14) and their implications for the thermohaline circulation. *Climate of the Past* 6, 531–552.
- Volkman, J.K., Eglinton, G., Corner, E.D.S., Sargent, J.R., 1980. Novel unsaturated straight-chain C_{37} – C_{39} methyl and ethyl ketones in marine sediments and a coccolithophorid *Emiliania huxleyi*. In: Douglas, A.G., Maxwell, J.R. (Eds.), *Advances in Organic Geochemistry*, 1979. Pergamon Press, Oxford, pp. 219–227.
- Wu, B.Y., Wang, J., 2002. Possible impacts of winter Arctic Oscillation on Siberian high, the East Asian winter monsoon and sea-ice extent. *Advances in Atmospheric Sciences* 19, 297–320.
- Ziegler, M., Lourens, L.J., Tuenter, E., Reichert, G.J., 2010. High Arabian Sea productivity conditions during MIS 13 – odd monsoon event or intensified overturning circulation at the end of the Mid-Pleistocene transition? *Climate of the Past* 6, 63–76.